

Temporal Cascade and Structural Modelling of EHRs for Granular Readmission Prediction

Bhagya Hettige
Monash University
bhagya.hettige@monash.edu

Weiqing Wang
Monash University
teresa.wang@monash.edu

Yuan-Fang Li
Monash University
yuanfang.li@monash.edu

Suong Le
Monash Health
suong.le@monashhealth.org

Wray Buntine
Monash University
wray.buntine@monash.edu

Abstract—Predicting (1) *when* the next hospital admission occurs and (2) *what* will happen in the next admission about a patient by mining electronic health record (EHR) data can provide granular readmission predictions to assist clinical decision making. Recurrent neural network (RNN) and point process models are usually employed in modelling temporal sequential data. Simple RNN models assume that sequences of hospital visits follow strict causal dependencies between consecutive visits. However, in the real-world, a patient may have multiple co-existing chronic medical conditions, i.e., multimorbidity, which results in a *cascade* of visits where a non-immediate historical visit can be most influential to the next visit. Although a point process (e.g., Hawkes process) is able to model a cascade temporal relationship, it strongly relies on a prior generative process assumption. We propose a novel model, **MEDCAS**, to address these challenges. **MEDCAS** combines the strengths of RNN-based models and point processes by integrating point processes in modelling visit types and time gaps into an attention-based sequence-to-sequence learning model, which is able to capture the temporal cascade relationships. To supplement the patients with short visit sequences, a structural modelling technique with graph-based methods is used to construct the markers of the point process in **MEDCAS**. Extensive experiments on three real-world EHR datasets have been performed and the results demonstrate that **MEDCAS** outperforms state-of-the-art models in both tasks.

Index Terms—Electronic health record analysis, Disease prediction, Point processes

I. INTRODUCTION

The rapid increase of Electronic health record (EHR) data collected at hospitals presents an opportunity for applying machine learning techniques for healthcare analysis [1]–[3]. EHRs form longitudinal sequences of patient visits. Each visit records a set of medical codes (e.g., diagnosis, procedure and medication codes) observed during the visit. Sequential disease prediction, which predicts *what* medical codes will be observed in the next visit, is a core task in personalised healthcare. In addition, the knowledge of *when* a patient’s next visit might occur allows hospitals to better allocate resources (e.g., beds, staff) and proactively reduce preventable readmissions [4]. Thus, the ability to make accurate predictions for both *when* and *what* aspects of future visits is important for personalised healthcare, which can produce *granular readmission predictions*. To the best of our knowledge, only a few studies simultaneously model both tasks [5], [6]. This work is motivated by the observation

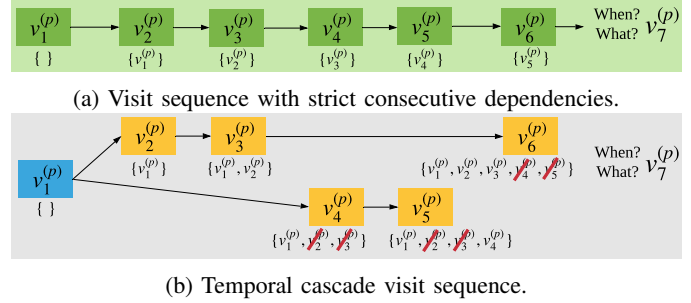


Fig. 1: Deconstructing the strict temporal dependencies between consecutive visits. Ancestor visits are shown within brackets.

that EHRs contain rich clinical information that can facilitate both tasks.

Most existing EHR modelling studies [5], [7] assume that a patient’s visit sequence follows strict causal dependencies between consecutive visits, so that each visit is influenced by its immediately preceding visit, as shown in Figure 1a. These techniques employ a chain structure to capture the memory effect of past visits. Prior research indicates that **multimorbidity** [8], which is defined as the co-occurrence of two or more chronic conditions, has moved onto the priority agenda for many health policymakers and healthcare providers [9], [10]. According to a global survey [10], the mean world multimorbidity prevalence for low and middle-income countries was 7.8%. Also, in Europe, patients with multimorbidity are some of the most costly and difficult-to-treat patients [9]. This prevalent and costly phenomenon induces complex causal relationships between visits where a non-immediate historical visit can be most influential to the next visit, as shown in Figure 1b. We term this effect “**temporal cascade relationships**”.

Attention based RNN models, such as Dipole [11] and RETAIN [12], are capable of modelling these temporal cascade relationships. However, they both regard visit sequences as evenly spaced time series and overlook the influence of time gaps between visits which is usually not the case in real-world medical data. Naturally, they cannot predict *when*. In contrast, temporal point processes naturally describe events that occur

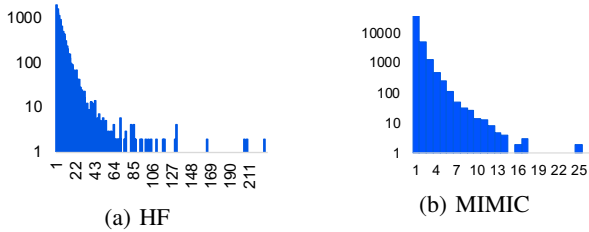


Fig. 2: $\log_{10}(\# \text{ patients})$ against visit sequence lengths.

in continuous time. Typical point process models, such as Hawkes [13], strongly rely on prior knowledge of the data distribution and the excitation process with strict parametric assumptions, which is usually not observed in the real-world. Neural point process models, such as RMTTP [14], capture these unknown temporal dynamics using RNN. Yet, they mimic the chained structure of event sequences to model historical memory effect, and are not capable of modelling the cascade relationships.

We propose a novel model, MEDCAS, to address these problems. MEDCAS combines the strengths of point process models and attention-based RNN models, and is able to capture the cascade relationships with time gap influences without a strong prior data distribution assumption. The basic idea of MEDCAS is to integrate point processes in learning visit type and time gap information into an attention-based RNN framework. Different from existing attention-based RNN models (e.g., Dipole [11] and RETAIN [12]) where attention is optimized for predicting *what* only, MEDCAS adopts a *time-aware* attention-based RNN encoder-decoder structure where the attention is learned not only in predicting *what*, but also in modelling the intensity to predict *when*. Thus, the cascade relationships for visit sequences captured by MEDCAS are also *time-aware* compared to existing EHR models where time is usually ignored. Moreover, a novel intensity function is introduced, so that no prior knowledge of the data and the excitation process is required for modelling cascade relationships, compared with existing point process models.

Many patients in EHR data have short medical histories, as shown in Figure 2 for two real-world datasets used in our experiments. Both distributions are highly imbalanced, with a median of 5 visits in HF and 1 visit in MIMIC. We term this problem the “cold start patient problem” in the healthcare domain. Inspired by the structural modelling technique proposed in MedGraph [7], MEDCAS encodes the visit-code relationships (Figure 3) to learn the local (within a patient) and global (across other patients) code-sharing behaviours of visits. With the globally captured visit similarities in terms of medical conditions across other patients, we can effectively alleviate the cold start patient problem in the absence of much temporal data about a patient.

The main contributions of this paper are threefold:

- 1) A granular readmission prediction model, MEDCAS, which (1) simultaneously predicts *when* the next visit occurs and *what* happens in the next visit (2) effectively

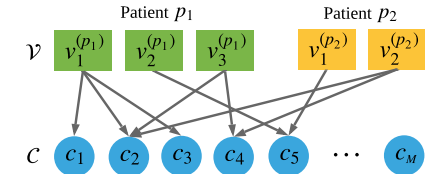


Fig. 3: Code-sharing behavior of visits.

models multimorbidity phenomenon without requiring prior knowledge about the EHR data distribution.

- 2) A novel architecture capable of modelling *time-gap aware cascade relationships* in patients’ visit sequences by integrating point process into an attention-based RNN encoder-decoder structure where the attention is learned for predicting not only *what* but also *when*. To generate visit markers for the point process effectively especially for the cold-start patients, a graph-based structure modelling method is adopted and a novel sampling method has been proposed to avoid cluttered joint training of structural and temporal parts accordingly.
- 3) An extensive experimental study conducted on three real-world EHR datasets that demonstrates the superiority of MEDCAS over state-of-the-art EHR models.

II. RELATED WORK

Over the years, many EHR modelling methods [1], [2], [15]–[19] have been proposed to leverage the patterns of patients, visits and codes to answer questions on predicting various medical outcomes of patients, such as next disease prediction [6], [11], [15]–[17], medical risk prediction [18]–[20] and mortality prediction [7], [21].

Med2Vec [20], a Skip-gram-based method [22], learns to predict codes of the future visit without temporal dependencies. Dipole [11] is an attention-based bi-directional RNN model that captures long-term historical visit dependencies for the prediction of the next visit’s codes. DoctorAI [5], also based on RNN, captures time gaps along with a disease prediction task, but still uses the chained structure of the visit sequences. RETAIN [12] is an interpretable predictive model with reverse-time attention. T-LSTM [23] implements a time-aware LSTM cell to capture the time gaps between visits. MiME [24] models the hierarchical encounter structure in the EHRs. But, the hierarchical granularity of medical codes is not always available in the real-world, thus it has limited usage. MedGraph [7], exploits both structural and temporal aspects in EHRs which uses a point process model [14] to capture the time gap irregularities, but fails to model the cascade relationships. GCT [21] models a graph to learn the implicit code relations using self-attention transformers, but ignores the temporal aspect of visits. ConCare [25] is another recent work which uses a transformer network to learn the temporal ordering of the visits. Some prominent baselines are compared in Table I.

Several recent studies [6], [7] have explored visit sequence modelling with marked point processes. Deep learning approaches [14], [26] have been developed to model the marked

TABLE I: Comparison with existing work (abbreviations: **ATTN** - attention on the past and **PP** - point process modelling).

EHR Modelling Method	Technique	Temporal	Cascades	Irregular time	Structural	Time + Disease
Med2Vec [20]	Skip-gram	×	×	×	✓	×
DoctorAI [5]	RNN	✓	×	×	×	✓
RETAIN [12]	RNN+ATTN	✓	✓	×	×	×
Dipole [11]	RNN+ATTN	✓	✓	×	×	×
T-LSTM [23]	RNN	✓	×	✓	×	×
MedGraph [7]	RNN+PP	✓	×	✓	✓	×
MEDCAS (ours)	RNN+PP+ATTN	✓	✓	✓	✓	✓

point processes which maximises the likelihood of observing the marked event sequences. CYAN-RNN [27] proposed a sequence-to-sequence approach to model the cascade dynamics in information diffusion networks, such as social-media post sharing.

III. METHODOLOGY

A. Problem Definition

The input data is a set of visit sequences $\{\mathcal{S}^{(1)}, \mathcal{S}^{(2)}, \dots, \mathcal{S}^{(P)}\}$ for P patients. For a patient p , his/her visit history denoted as $\mathcal{S}^{(p)} = \{v_i^{(p)} = (t_i^{(p)}, \mathbf{x}_i^{(p)})\}_{i=1}^{N^{(p)}}$ consists of a temporally ordered sequence of tuples of $N^{(p)}$ finite timesteps with $i \in \mathbb{Z}^+$, where $v_i^{(p)}$ is the i -th visit of patient p , in which $t_i^{(p)} \in [0, +\infty)$ is the visit's timestamp, and $\mathbf{x}_i^{(p)}$ denotes the set of medical codes (i.e., diagnosis and procedure codes) associated with the visit. $\mathbf{x}_i^{(p)} \in \{0, 1\}^{|\mathcal{C}|}$ is a multi-hot binary vector which marks the occurrence of medical codes from taxonomy $\mathcal{C} = \{c_1, c_2, \dots, c_{|\mathcal{C}|}\}$ in the visit. Given a patient p 's visit history up to timestep $t_i^{(p)}$, our task is to answer the following questions about p 's next visit, $v_{i+1}^{(p)}$:

- 1) *when* will the next visit happen?
- 2) *what* (i.e., medical codes) will happen in the next visit?

B. MEDCAS Architecture

Without loss of generality, we present MEDCAS for a single patient. The overall architecture of MEDCAS is shown in Figure 4. Given a patient's visit sequence from timestep 1 to i , our task is to predict the *time* and *diseases* of the next visit, i.e., $(t_{i+1}, \mathbf{x}_{i+1})$. Using this input visit sequence, we model a point process to capture the time gap influences of the past visits. First, we transform each \mathbf{x}_i into a latent visit vector, $\mathbf{v}_i \in \mathbb{R}^{D_m}$, by exploiting the graph structural visit-code relationships in EHR, shown in Figure 3. This \mathbf{v}_i will be used as the marker in the point process. Then, we construct a time-context vector, $\boldsymbol{\tau}_i$, with a linear transformation to effectively model the time gap irregularities between consecutive visits. Using the marker \mathbf{v}_i and the time-context $\boldsymbol{\tau}_i$ vectors, we model the temporal *cascade relationships* through a time-aware attention-based encoder-decoder alignment model. At the i -th timestep, the alignment model predicts the time and the diseases of the next visit $(t_{i+1}, \mathbf{x}_{i+1})$. To align the input and the output visit sequences, we employ an aggregated attention-based ancestor-context vector \mathbf{z}_i , which computes the attention of each historical visit on the next visit. This ancestor-context

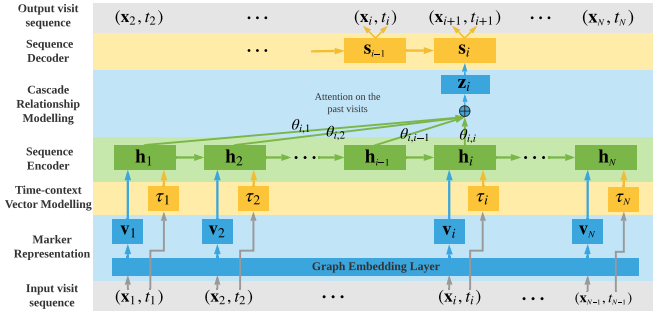


Fig. 4: The MEDCAS architecture.

vector models the implicit cascade relationships. Accordingly, we define the intensity function which models the temporal cascade relationships of the visit sequences using both causal and implicit temporal relationships. Since we jointly optimise ancestor visit alignment and the point process intensity, the modelled temporal cascade relationships learned via attention are *time-informed*.

1) *Marker Representation*: Existing point process modelling methods [14], [27] capture sequences of events with a one-hot marker, unsuitable to represent visits which typically have multiple medical codes, i.e., high-dimensional, sparse multi-hot vectors \mathbf{x}_i .

Graph embedding layer: A naïve approach to deal with simultaneous event types is to encode the multi-hot codes into a latent representation before feeding into the temporal model. However, this simple encoding is unable to capture the complex *local* (codes connected to a visit) and *global* (visits sharing similar codes) code-sharing behaviours of visits. Inspired by the bipartite graph technique proposed in MedGraph [7] to capture visit-code relationships, we construct an unweighted bipartite graph $G = (\mathcal{V} \cup \mathcal{C}, E)$, where $\mathcal{V} = \{v_1, v_2, \dots, v_N\}$ is the visit node partition, \mathcal{C} is the code node partition, and E is the set of edges between them (Figure 3). E can be constructed from the multi-hot code vector \mathbf{x}_i for each visit node v_i .

Attributed nodes enable inductive inference of future/unseen visits [28]. For visit v_i 's attribute vector, we use \mathbf{x}_i which denotes the codes in v_i , since it can uniquely distinguish each visit. A one-hot vector is used for representing code nodes as we do not use supplementary code data. i.e., $\mathbf{m}_j \in \mathbf{I}_{|\mathcal{C}|}$ where $\mathbf{I}_{|\mathcal{C}|}$ is the identity matrix, is used as the attribute vector of each code c_j . We use an attributed graph embedding method to learn the visit-code relationships to obtain visit and code embeddings. In this work, we use the second-order proximity [29] to capture visit neighbourhood similarity.

Let $(v_i, c_j) \in E$ be an edge between visit v_i and code c_j

with attributes $\mathbf{x}_i \in \{0, 1\}^{|\mathcal{C}|}$ and $\mathbf{m}_j \in \{0, 1\}^{|\mathcal{C}|}$, respectively. We project the two node types to a common semantic latent space using two transformation functions parameterised by $\mathbf{W}_v, \mathbf{W}_c \in \mathbb{R}^{D_m \times |\mathcal{C}|}$, $\mathbf{b}_v, \mathbf{b}_c \in \mathbb{R}^{D_m}$, where D_m is the dimension of the latent vector.

$$\mathbf{v}_i = \mathbf{W}_v^T \mathbf{x}_i + \mathbf{b}_v \quad \text{and} \quad \mathbf{c}_j = \mathbf{W}_c^T \mathbf{m}_j + \mathbf{b}_c \quad (1)$$

We define the probability that the patient is diagnosed with disease c_j during hospital visit v_i as the conditional probability of code c_j generated by visit v_i as: $p(c_j|v_i) = \frac{\exp(\mathbf{c}_j^T \cdot \mathbf{v}_i)}{\sum_{c_j \in \mathcal{C}} \exp(\mathbf{c}_j^T \cdot \mathbf{v}_i)}$. For each visit $v_i \in \mathcal{V}$, $p(\cdot|v_i)$ defines the conditional distribution over all the codes in \mathcal{C} , so that the visit's neighbourhood is modeled by this formulation. We define the empirical probability of observing code c_j in visit v_i as $\hat{p}(c_j|v_i) = \frac{1}{\text{degree}(v_i)} = \frac{1}{\text{sum}(\mathbf{x}_i)}$. Therefore, to preserve the second-order proximity for visit node v_i , the conditional probability $p(\cdot|v_i)$ and the empirical probability $\hat{p}(\cdot|v_i)$ need to be closer. By applying Kullback Leibler (KL) divergence and omitting the constants [29], we can derive the structural loss for the visit-code graph as:

$$\mathcal{L}_s = - \sum_{(v_i, c_j) \in E} \log p(c_j|v_i) \quad (2)$$

We use the visit embedding \mathbf{v}_i , which captures the code-sharing behaviours, as the latent marker of the i -th visit.

2) *Time-context Vector Modelling*: To model the point process, we need to define the time-context of events. Accordingly, for each visit we consider its time gap from the immediately previous visit. Since time gaps are irregular and spans from hours to years in EHR systems, we transform this time gap to a log scaled value, so for timestep i , $\Delta_i = \log(t_i - t_{i-1})$. Existing approaches simply concatenate this scalar time value to the marker vector. However, when the event marker vector is high-dimensional, it is likely that the model will ignore the effects of a scalar time-context value, which has been experimentally validated in the ablation analysis. Thus, we convert this scalar into a high-dimensional vector to capture the time gap irregularities more effectively. We use a linear transformation, due to its simplicity and experimentally validated effectiveness, to construct time gap vectors $\boldsymbol{\tau}_i = \mathbf{W}_\Delta \cdot \Delta_i \in \mathbb{R}^{D_t}$, where D_t is the time-context vector dimension. The linear transformation $\mathbf{W}_\Delta \in \mathbb{R}^{D_t \times 1}$ is initialised with a 0-mean Gaussian.

3) *Sequence Encoder*: The encoder reads the input visit sequence up to timestep i . MEDCAS constructs the hidden state vector of the timestep i using an RNN with D units as:

$$\mathbf{h}_i = \text{RNN}(\mathbf{h}_{i-1}, [\mathbf{v}_i, \boldsymbol{\tau}_i]) \quad (3)$$

Intuitively, the sequence encoder captures the history of the patient in a chained structure. For each timestep i , we concatenate the marker vector \mathbf{v}_i and the time-context vector $\boldsymbol{\tau}_i$ as input to the RNN along with the previous hidden state. As a result, \mathbf{h}_i carries *time-aware memory* on the patient's medical disease progression up to timestep i .

4) *Cascade Relationship Modelling*: MEDCAS identifies the candidate ancestor visits at timestep i using an attention-based scheme. The ancestor visits are aggregated into an ancestor-context vector \mathbf{z}_i weighted by their attention. Different from NMT models, we restrict that only the visits up to i are considered as ancestors of the next visit at $i + 1$.

$$\mathbf{z}_i = \sum_{j=1}^i \theta_{i,j} \cdot \mathbf{h}_j \quad (4)$$

where $\theta_{i,j} \geq 0$ with $\sum_{j=1}^i \theta_{i,j} = 1$ is the likelihood of the visit v_j being an influential visit for the next visit. Since the output of timestep i is v_{i+1} in the decoder, this gives the likelihood of v_j being an ancestor visit of the visit v_{i+1} in the cascade relationship setting. The attention score is defined with the decoder hidden state which is used to align the input visit sequence to the output visit sequence.

5) *Sequence Decoder*: In the RNN decoder with D units, we feed the previous decoder hidden state \mathbf{s}_{i-1} , encoder input of current timestep \mathbf{x}_i (i.e., the teacher forcing learning scheme) and ancestor-context vector \mathbf{z}_i to construct the *latent cascading state* at the current timestep \mathbf{s}_i as:

$$\mathbf{s}_i = \text{RNN}(\mathbf{s}_{i-1}, \mathbf{x}_i, \mathbf{z}_i) \quad (5)$$

We define an alignment score for each historical visit at timestep j and the output visit at timestep i (since we let the output sequence to be one timestep ahead of the input sequence, output at timestep $(i + 1)$ is the input at timestep i) as: $\mathbf{e}_{i,j} = a(\mathbf{s}_{i-1}, \mathbf{h}_j)$, where a is a feedforward network which is jointly trained with the complete model. The attention weight to model the cascade relationships is defined as:

$$\theta_{i,j} = \frac{\exp(\mathbf{e}_{i,j})}{\sum_{k=1}^i \exp(\mathbf{e}_{i,k})} \quad (6)$$

6) *Output Visit Sequence*: The two tasks of MEDCAS are to predict, (1) *when* will the $(i + 1)$ -th visit happen, and (2) *what* will happen in the $(i + 1)$ -th visit. We use the decoder hidden state at timestep i , \mathbf{s}_i , as the latent vector of the $(i + 1)$ -th visit to make these predictions. For disease prediction:

$$\hat{\mathbf{x}}_{i+1} = \text{Softmax}(\mathbf{W}_o \mathbf{s}_i + \mathbf{b}_o) \quad (7)$$

where $\mathbf{W}_o^T \in \mathbb{R}^{|\mathcal{C}| \times D}$, $\mathbf{b}_o \in \mathbb{R}^{|\mathcal{C}|}$, and D is the dimension of the decoder hidden state, \mathbf{s}_i . We use categorical cross-entropy between the actual and the predicted codes as the loss for disease prediction.

$$\mathcal{L}_{d(i)} = -(\mathbf{x}_{i+1}^\top \cdot \log(\hat{\mathbf{x}}_{i+1}) + (1 - \mathbf{x}_{i+1})^\top \cdot \log(1 - \hat{\mathbf{x}}_{i+1})) \quad (8)$$

To model the point process, a novel intensity function with temporal cascade relationships is defined as:

$$\lambda^*(t) = \exp \left(\underbrace{\mathbf{W}_h^\top \mathbf{h}_t}_{\text{explicit temporal influence}} + \underbrace{\mathbf{W}_s^\top \mathbf{s}_t}_{\text{implicit cascade influence}} + \underbrace{\mathbf{W}_u^\top \mathbf{v}_t}_{\text{current visit influence}} + \underbrace{W_t(t - t_i)}_{\text{current time influence}} + \underbrace{b_t}_{\text{base intensity}} \right) \quad (9)$$

where $\mathbf{W}_h, \mathbf{W}_s \in \mathbb{R}^{D \times 1}$, $\mathbf{W}_u \in \mathbb{R}^{D_m \times 1}$ and $W_t, b_t \in \mathbb{R}$. Using this intensity function, we define the likelihood that

the next visit event will occur at a predicted time t using the conditional density function [14]:

$$p(t|\mathbf{x}_i, \mathbf{z}_i, \mathbf{s}_i) = f^*(t) = \lambda^*(t) \exp\left(-\int_{t_i}^t \lambda^*(\tau) d\tau\right) \quad (10)$$

This likelihood of observing the next visit at the ground truth time t_{i+1} in the training data should be maximised to learn the temporal cascade relationships. Specifically, we minimise the negative log likelihood for time modelling as:

$$\mathcal{L}_{t(i)} = -\log\left(p(t_{i+1}|\mathbf{x}_i, \mathbf{z}_i, \mathbf{s}_i)\right) \quad (11)$$

Once the model is trained, to predict the time of the next visit at timestep $i + 1$, we adopt the expectation formula [14]:

$$\hat{t}_{i+1} = \int_{t_i}^{\infty} t \cdot f^*(t) dt \quad (12)$$

7) *Overall Loss Function:* For P patients we define the overall loss (Eqs. 2, 8, 11) with hyperparameters $\alpha, \beta > 0$:

$$\mathcal{L}(\{\mathcal{S}^{(p)}\}_{p=1}^P) = \frac{1}{P} \sum_{p=1}^P \left(\frac{\sum_{i=1}^{N^{(p)}} (\mathcal{L}_{d(i)}^{(p)} + \alpha \mathcal{L}_{t(i)}^{(p)}) + \beta \mathcal{L}_s^{(p)}}{N^{(p)}} \right) \quad (13)$$

C. Model Optimisation

MEDCAS jointly optimises both structural and temporal aspects in an end-to-end framework. It connects the two parts, by feeding the visit embedding encoded by the structural part as the marker of the point process in the temporal part.

For the structural part, a naïve edge sampling method that is independent of the temporal sequence sampling will be completely random. More specifically, the structural part will select visit-code pairs that are distinct from the patients sampled by the temporal part in each minibatch. Such distinct visit-code samples can deviate the model when updating the parameters in the optimisation phase. To mitigate this issue, we propose a novel **visit-sequence-based edge sampling** method to ensure that the visit-code relations we learn are related to the sampled set of patients. We first sample a batch of patients for the temporal part. Then, for the structural part, we use the visits in these patients to sample the visit-code edges as the set of positive edges, thus removing the randomness of positive edge sampling to avoid cluttered joint training for the two components. Given the sampled positive edges, we randomly select K negative edges for each positive edge by fixing the visit node for the structural component. This new sampling approach has been experimentally validated to be effective in our Ablation Analysis.

IV. EXPERIMENTS

We evaluate the performance of MEDCAS on three real-world EHR datasets and compare against several state-of-art EHR machine learning methods. Source code is available through this link: <https://bit.ly/3hvo0IV>. All the experiments were performed on a MacBook Pro laptop with 16GB memory and a 2.6 GHz Intel Core i7 processor.

TABLE II: Statistics of the real-world EHR datasets.

Dataset	HF	CL	MIMIC
Total # patients	10,713	3,830	7,499
Total # visits	204,753	122,733	19,911
Avg. # visits per patient	18.51	29.84	2.66
Medical Codes			
Total # unique codes	8,541	8,382	8,993
Avg. # codes per visit	5.55	5.05	16.92
Max # codes per visit	83	94	62
CCS Grouped Medical Codes			
Total # unique codes	249	248	294
Avg. # codes per visit	3.02	2.82	13.10
Max # codes per visit	33	37	14

A. Experimental Settings

1) *Datasets:* Two real-world proprietary cohort-specific EHR datasets: heart failure (HF) and chronic liver disease (CL), and one public ICU EHR dataset: MIMIC¹ are used. MIMIC is chosen to ensure the reproducibility on publicly available datasets. The two chronic diseases, HF and CL, are chosen as most patients with these disease tend to exhibit multimorbidity [8].

We filter out the patients with only one visit. Brief statistics of the three datasets are shown in Table II. Both proprietary datasets are from the same hospital which use *ICD-10 medical codes*. MIMIC uses *ICD-9 medical codes*. Also, we can categorise the medical codes in accordance with the corresponding clinical classification software (CCS)², which divides the codes into clinically meaningful groups, to reduce the dimensionality in training (Eq. 8). We randomly split patient sequences in each dataset into train:validation:test with a 80:5:15 ratio.

2) *Compared Algorithms:* Different state-of-art techniques on time and disease prediction are compared.

Time prediction: Three state-of-the-art time models are compared. **DoctorAI** [5] is a RNN-based encoder model which is able to predict both time and medical codes of the next visit by exploiting the chained memory structure in visits. **Homogeneous Poisson Process (HPP)** [30] is a stochastic point process model where the intensity function is a constant. It produces an estimate of the average inter-visit gaps. **Hawkes Process (HP)** [13] is a stochastic point process model that fits the intensity function with an exponentially decaying kernel $\lambda^*(t) = \mu + \alpha \sum_{t_i < t} \exp(-\beta(t - t_i))$. Considering time prediction as a regression task, we train a **linear regression model (LR)** and a **XGBoost regression model (XGBR)** with combination of input features: raw visit features \mathbf{x}_i (i.e., medical code multi-hot vector at timestep i), visit embeddings emb_i^{visit} (i.e., marker representation vector \mathbf{v}_i at timestep i) and patient embeddings emb_i^{pat} (i.e., decoder state vector \mathbf{s}_i at timestep i) learned from MEDCAS.

Disease prediction: Five state-of-the-art EHR methods are compared: **Med2Vec**, **DoctorAI**, **RETAIN**, **Dipole T-LSTM**

¹<https://mimic.physionet.org>

²https://hcup-us.ahrq.gov/toolssoftware/ccsr/ccs_refined.jsp

TABLE III: Time prediction performance. RMSE of log time. \mathbf{x}_i is the medical code vector of the current visit, emb_i^{visit} is the MEDCAS visit embedding vector and emb_i^{pat} is the MEDCAS patient embedding vector (more details in Compared Algorithms).

Algorithm	HF	CL	MIMIC
HPP	3.5916	3.5279	4.9734
HP	3.2410	3.5613	4.4706
DoctorAI	1.8312	1.9053	1.6273
LR (\mathbf{x}_i)	8.2E+4	7.6E+9	4.8E+10
LR (emb_i^{visit})	2.3659	2.2590	1.5628
LR (emb_i^{pat})	2.0094	1.8663	1.4668
LR ($emb_i^{visit} + emb_i^{pat}$)	2.0029	1.8579	1.4303
LR ($\mathbf{x}_i + emb_i^{visit}$)	2.3702	2.2641	1.5431
LR ($\mathbf{x}_i + emb_i^{pat}$)	2.0051	1.8593	1.3963
LR ($\mathbf{x}_i + emb_i^{visit} + emb_i^{pat}$)	2.0060	1.8606	1.4079
XGBR (\mathbf{x}_i)	2.3657	2.2609	1.5188
XGBR (emb_i^{visit})	2.3717	2.2679	1.5639
XGBR (emb_i^{pat})	2.0281	1.8909	1.4461
XGBR ($emb_i^{visit} + emb_i^{pat}$)	2.0294	1.8844	1.4294
XGBR ($\mathbf{x}_i + emb_i^{visit}$)	2.3709	2.2627	1.5328
XGBR ($\mathbf{x}_i + emb_i^{pat}$)	2.0298	1.8962	1.4139
XGBR ($\mathbf{x}_i + emb_i^{visit} + emb_i^{pat}$)	2.0265	1.8706	1.4172
MEDCAS	1.7091	1.6950	1.3950

and **MedGraph**, which have been discussed in the Related Work section. The main differences are summarized in Table I.

3) *Evaluation Metrics*: For the time prediction task, root mean squared error (RMSE) is used as the evaluation metric. For the disease prediction task, Recall@k and AUC scores are used to evaluate model performance. Since the disease prediction task is a multi-label classification task, AUC score can be used to (micro-)average over all medical code classes. On the other hand, the disease prediction task can also be evaluated as an item ranking task as we can rank the predicted codes in each visit based on the probability scores obtained with our model. Recall@k computes the ratio of the number of relevant codes in the ranked top- k predicted codes in the total number of actually present codes.

4) *Hyperparameter Settings*: We set the visit embedding dimension (D_m in MEDCAS) in all the methods to 128. In our model, we fix $\alpha = 0.01$ and $\beta = 100$ in all three datasets based on the validation set. We fix the number of negative codes randomly selected per positive code as $K = 2$. Based on the validation set, we fix the size of time-context vector embedding to be 8 in HF, 64 in CL and 128 in MIMIC. We use an Adam optimizer with a fixed learning rate of 0.001. For regularization in MEDCAS we use L2 norm with a coefficient of 0.001. We run each algorithm 100 epochs with a batch size of 128 and report their best performance across all the epochs.

B. Time Prediction: When will it happen?

We predict the log-scaled time interval between the current visit and the next visit and report the RMSE in Table III for all three datasets. The lower the RMSE, the better the

time prediction performance is. Since the time gaps between consecutive visits of a patient can be highly irregular, the time to the next visit can be extremely skewed. Therefore, similarly to DoctorAI [5], we compute the RMSE in predicting the log scaled time value to mitigate the effect of the irregular time durations in the RMSE metric in all the compared models.

MEDCAS is the best in predicting *when* the next visit occurs on all the datasets, by leveraging the temporal cascade relationship modelling and structural code-sharing behaviour modelling. The parametric point process models, HPP and HP, perform the worst because of the fixed parametric assumptions they make about the generative process (constant intensity of HPP and exponential kernel of HP). On the other hand, both sequential deep learning models (i.e., MEDCAS and DoctorAI) demonstrate superiority in predicting the time of next visit by learning the complex temporal relationships in the presence of additional information on visits, i.e., medical codes. MEDCAS has a very obvious improvements compared to DoctorAI, as DoctorAI only encodes the causal sequential ordering in a chained structure of visits using an RNN. In contrast, MEDCAS models the varying influences of ancestor visits via point process modelling and captures the implicit temporal cascade relationships through attention.

Then, we compare the classic regression models (i.e., LR and XGBR) trained with different combinations of input features (i.e., the raw features, visit embeddings learned by MEDCAS and patient embeddings learned by MEDCAS). Based on the results, there are two major observations, (1) the raw features (\mathbf{x}_i) and the visit embeddings (emb_i^{visit}) do not perform well in both LR and XGBR, and (2) the patient embedding (emb_i^{pat}) perform well in these two methods. The patient embedding learned via MEDCAS has accumulated time information along with the longitudinal historical visits. But, the raw features and the visit embeddings only have the medical code co-location information and do not capture the temporal information from the visit sequences. Therefore, the results show that the inclusion of time context through the patient embedding improves the performance of time prediction task across all the datasets. However, MEDCAS outperforms the two simple regression models. This shows that the combined effect of structural and temporal learning with point process based time estimation using Eq. 12 in MEDCAS is effective.

C. Disease Prediction: What will happen?

We report the Recall@k and AUC scores on the disease prediction task on the three datasets in Table IV.

As can be seen from the results, MEDCAS achieves the best performance on both recall and AUC across all three datasets, in particular showing significantly higher Recall@k for all k . MEDCAS achieves better performance over the existing attention-based encoder models (i.e., RETAIN and Dipole) due to two possible reasons. One reason is that RETAIN and Dipole learn attention by computing the relative importance of past visits on the current visit instead of the next visit. The other possible reason is that MEDCAS learn the attention more accurately compared with RETAIN and Dipole as it leverages

TABLE IV: Disease prediction performance.

Algorithm	HF				CL				MIMIC			
	Recall@k				Recall@k				Recall@k			
	k=10	k=20	k=30	AUC	k=10	k=20	k=30	AUC	k=10	k=20	k=30	AUC
Med2Vec	0.5735	0.7136	0.7945	0.9301	0.6414	0.7547	0.8232	0.9413	0.3017	0.4603	0.5666	0.8791
DoctorAI	0.5006	0.6381	0.7132	0.7567	0.6011	0.7341	0.8117	0.8461	0.3026	0.4607	0.5659	0.7406
RETAIN	0.5495	0.6867	0.7646	0.9214	0.6183	0.7319	0.7918	0.9281	0.2573	0.4135	0.5262	0.8643
Dipole	0.5555	0.6942	0.7751	0.9254	0.6487	0.7610	0.8246	0.9403	0.3218	0.4819	0.5878	0.8781
T-LSTM	0.3509	0.5554	0.6858	0.8275	0.3747	0.5477	0.7100	0.8508	0.2067	0.3878	0.5435	0.8279
MedGraph	0.5514	0.6950	0.7793	0.9277	0.6601	0.7693	0.8331	0.9421	0.2998	0.4577	0.5671	0.8779
MEDCAS	0.6118	0.7419	0.8107	0.9373	0.6832	0.7893	0.8445	0.9479	0.3350	0.4901	0.5928	0.8816

both *what* and *when* aspects in modelling the patient sequences. Another observation is that the EHR graph structure learning methods, MEDCAS and MedGraph, perform well in disease prediction as they explicitly optimise for the code-sharing similarity of visits.

Moreover, disease prediction on MIMIC gives lower accuracy when compared with the other two. This is because of the substantially shorter visit sequences in MIMIC, which provides less information for a model to learn from about a patient (i.e., cold start patient problem). Additionally, HF and CL are cohort-specific EHR datasets and the disease progression patterns of the patients will be fairly similar when compared to generic ICU admission in MIMIC.

D. Performance Analysis on Cold Start Patients

As shown in Figure 2, many patients have short medical histories, with a median of 5 visits in HF and 1 visit in MIMIC. Intuitively, these short histories will make the accurate patient sequence modelling challenging. We refer this challenge as the “cold start patient problem”. In this section, we evaluate our model against the baselines to analyse their effectiveness in dealing with the cold start patient problem. We report the results on MIMIC and the results on HF and CL datasets have similar trends.

For the patient sequences in the test set, we first remove the patients with only one visit and divide the patients into four partitions according to the length of patient sequences. Let x be the length of patient sequences. We define the partitions as: $x \in (0, 2]$, $(2, 5]$, $(5, 10]$ and $(10, 20]$. We report the results on time and disease prediction in Figure 5a– 5b.

In both tasks, the longer the visit sequence is, the better the performance is for all the compared models. For the time prediction task, MEDCAS is performing the best for cold start patients as it can utilize the global code-sharing behaviour of visits of similar patients when the patient has short history. MEDCAS shows significantly better recall scores across all sequence partitions for disease prediction task. Again, we can attribute this performance gain to the structure learning component, which is further validated by the second-best performing model, MedGraph which also models the code-sharing structure. RETAIN’s performance is almost the worst as its reverse-time attention mechanism with two RNN structures.

TABLE V: Ablation analysis: time and disease prediction.

Variant	Time		Disease			
	version	RMSE	Recall@k			
			k=10	k=20	k=30	AUC
MEDCAS-1	1.404	0.3135	0.4709	0.5780	0.8775	
MEDCAS-2	1.401	0.3105	0.4616	0.5641	0.8735	
MEDCAS-3	1.405	0.3295	0.4831	0.5861	0.8790	
MEDCAS-4	1.402	0.3276	0.4814	0.5812	0.8783	
MEDCAS-5	1.400	0.3261	0.4832	0.5855	0.8792	
MEDCAS	1.395	0.3350	0.4901	0.5928	0.8816	

When the sequences are shorter, RETAIN does not benefit from the reverse-time attention scheme and finds it difficult to infer a correct prediction.

E. Ablation Analysis

An extensive ablation study has been conducted to evaluate the effectiveness of each proposed component in MEDCAS on both disease and time prediction tasks (Table V). Due to the limited space, the ablation study is only reported on MIMIC. Five variant versions of MEDCAS are compared.

MEDCAS-1: without cascade modelling. It assumes that each visit is only affected by the immediate previous visit and no attention is learned. **MEDCAS-2:** without visit-code graph structural modelling. It uses a jointly learned feedforward network to encode the multi-hot visit vectors (\mathbf{x}_i) into a latent marker. **MEDCAS-3:** without time-context vector modelling. It directly concatenates the log-scaled time gap value Δ_i with the latent marker vector as the input to the sequence encoder. **MEDCAS-4:** without visit-sequence-based edge sampling, where the model randomly samples positive edges and K negative edges for each positive edge. **MEDCAS-5:** with a single-parent visit instead of multiple ancestor visits to approximate a classic Hawkes process. Classic Hawkes process models assume that an event is affected by a single parent event in the history. The attention score function is modified to $\theta_{i,j} = \{0, 1\}$, $\sum_{j=1}^i \theta_{i,j} = 1$ so that only one past visit is chosen as the parent.

Based on the results reported in Table V, we can see that MEDCAS full model outperforms all the variants on both tasks, which validate the effectiveness of the five components in our model. The consistent performance degradation for both tasks in

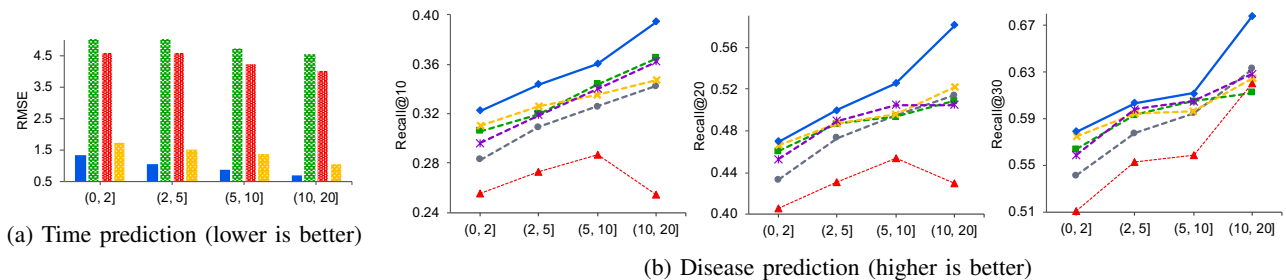


Fig. 5: The cold start patient problem: time and disease prediction performance of cold start patient sequences measured (y-axis) in terms of patient sequence lengths (x-axis) in MIMIC.

MEDCAS-1 and MEDCAS-5 compared with MEDCAS validates the effectiveness of modelling temporal cascade relationships in patient visit sequences. Note that, although both MEDCAS-1 and MEDCAS-5 assume that each visit is affected by one single parent visit, MEDCAS-5 outperforms MEDCAS-1 consistently. The reason is that MEDCAS-5 learns to choose the parent visit from all the history visits while MEDCAS-1 limits the parent visit to be the immediate previous visit. Moreover, the consistent performance gap between MEDCAS-5 and MEDCAS validates that each visit can be affected by multiple previous visits.

For time prediction, the performance gap between MEDCAS and MEDCAS-3 where time-context vector learning is removed, is the largest. This shows that time-context vector is very beneficial for time prediction as it adds an extra depth of information along the time axis. For disease prediction, the performance gap between MEDCAS and MEDCAS-2 where structure learning is removed is the largest. This demonstrates that the graph-based based code-sharing behaviour learning is very useful in this task. Moreover, the performance degradation of MEDCAS-1 is the second largest which shows the importance of temporal cascade modelling to account for multimorbidity in disease prediction.

F. Parameter Sensitivity Analysis

We study the sensitivity of α , β , marker embedding dimension and time-context embedding dimension in MEDCAS. The results on time and disease prediction tasks on MIMIC are shown in Figure 6. Larger α values improve time prediction performance (Fig. 6a) but decrease disease prediction accuracy (Fig. 6b), as α controls the relative weight of temporal learning as defined in Eq. 13 (optimal at $\alpha = 0.01$). When β increases, both the time (Fig.6c) and disease (Fig.6d) prediction performances improves, which demonstrates the contribution of the structural learning component in the two tasks (optimal at $\beta = 100$).

We analyse the trade-off of the marker embedding and the time embedding dimensions in Figure 6e and Figure 6f. In both settings, we keep the other dimension fixed at 128 and change the dimension under study. The model performs increasingly well until 128 (resp. 128) in the disease prediction task with increasing marker (resp. time) embedding dimension while keeping the time (resp. marker) embedding fixed. Time prediction performance also increases with marker (resp. time) embedding dimension and the best time accuracy is at 1024.

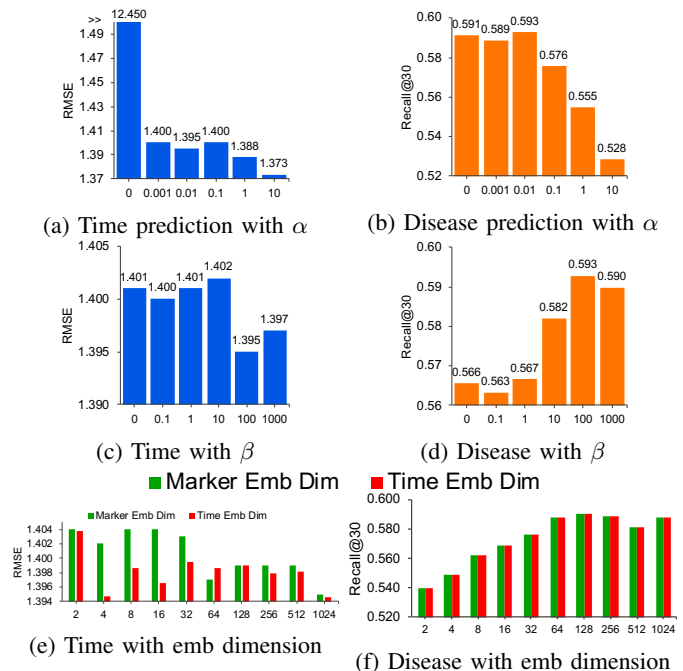


Fig. 6: Parameter sensitivity. Lower the better in Figs. (a), (c) and (e). Higher the better in Figs. (b), (d) and (f).

Considering performance of both tasks, the optimal marker dimension at 128 and time-context dimension at 128 for MIMIC can be observed.

V. CONCLUSION

EHR data can be used for fine-grained readmission prediction in answering *when* will the next visit occur and *what* will happen in the next visit. We presented MEDCAS, a novel temporal cascade and structural modelling framework for EHRs to simultaneously predict the time and the diseases of the next visit. MEDCAS combines point processes and RNN-based models to capture multimorbidity condition in patients by learning the inherent time-gap-aware cascade relationships via attention in the visit sequences. The structural aspect of EHRs is leveraged with a graph structure based technique to alleviate the cold start patient problem in EHRs. MEDCAS demonstrates significant performance gain over several state-of-the-art models in predicting time and diseases of the next visit across three real-world EHR datasets.

REFERENCES

- [1] B. Shickel, P. Tighe, A. Bihorac, and P. Rashidi, "Deep EHR: A survey of recent advances in deep learning techniques for electronic health record (EHR) analysis," *IEEE Journal of Biomedical and Health Informatics*, vol. 22, no. 5, pp. 1589–1604, 2017.
- [2] B. A. Goldstein, A. M. Navar, M. J. Pencina, and J. Ioannidis, "Opportunities and challenges in developing risk prediction models with electronic health records data: a systematic review," *JAMIA*, vol. 24, no. 1, pp. 198–208, 2017.
- [3] P. Yadav, M. S. Steinbach, V. Kumar, and G. J. Simon, "Mining electronic health records (EHRs): A survey," *ACM Comput. Surv.*, vol. 50, no. 6, pp. 1–40, 2018.
- [4] D. Kansagara, H. Englander, A. Salanitro, D. Kagen, C. Theobald, M. Freeman, and S. Kripalani, "Risk Prediction Models for Hospital Readmission: A Systematic Review," *JAMA*, vol. 306, no. 15, pp. 1688–1698, 2011.
- [5] E. Choi, M. T. Bahadori, A. Schuetz, W. F. Stewart, and J. Sun, "Doctor AI: predicting clinical events via recurrent neural networks," in *MLHC*, 2016.
- [6] Z. Qiao, S. Zhao, C. Xiao, X. Li, Y. Qin, and F. Wang, "Pairwise-ranking based collaborative recurrent neural networks for clinical event prediction," in *IJCAI*, 2018.
- [7] B. Hettige, W. Wang, Y. Li, S. Le, and W. L. Buntine, "MedGraph: structural and temporal representation learning of electronic medical records," in *ECAI*, 2020.
- [8] J. Almirall and M. Fortin, "The coexistence of terms to describe the presence of multiple concurrent diseases," *Journal of Comorbidity*, vol. 3, no. 1, pp. 4–9, 2013.
- [9] R. Navickas, V.-K. Petric, A. Feigl, and M. Seychell, "Multimorbidity: What Do We Know? What Should We do?" *Journal of Comorbidity*, vol. 6, no. 1, pp. 4–11, 2016.
- [10] S. Afshar, P. Roderick, P. Lowal, B. Dimitrov, and A. Hill, "Multimorbidity and the inequalities of global ageing: a cross-sectional study of 28 countries using the World Health Surveys," *BMC Public Health*, vol. 15, no. 1, p. 776, 2015.
- [11] F. Ma, R. Chitta, J. Zhou, Q. You, T. Sun, and J. Gao, "Dipole: Diagnosis prediction in healthcare via attention-based bidirectional recurrent neural networks," in *ACM SIGKDD*, 2017.
- [12] E. Choi, M. T. Bahadori, J. Sun, J. Kulas, A. Schuetz, and W. F. Stewart, "RETAIN: an interpretable predictive model for healthcare using reverse time attention mechanism," in *NIPS*, 2016.
- [13] A. G. Hawkes, "Spectra of some self-exciting and mutually exciting point processes," *Biometrika*, vol. 58, no. 1, pp. 83–90, 1971.
- [14] N. Du, H. Dai, R. Trivedi, U. Upadhyay, M. Gomez-Rodríguez, and L. Song, "Recurrent marked temporal point processes: Embedding event history to vector," in *ACM SIGKDD*, 2016.
- [15] J. Gao, X. Wang, Y. Wang, Z. Yang, J. Gao, J. Wang, W. Tang, and X. Xie, "CAMP: Co-Attention Memory Networks for Diagnosis Prediction in Healthcare," in *ICDM*, 2019.
- [16] J. Gao, X. Wang, Y. Wang, Z. Yang, J. Gao, J. Wang, W. Tang, and X. Xie, "CAMP: co-attention memory networks for diagnosis prediction in healthcare," in *ICDM*, 2019.
- [17] M. Zhang, C. R. King, M. Avidan, and Y. Chen, "Hierarchical attention propagation for healthcare representation learning," in *ACM SIGKDD*, 2020.
- [18] C. Yin, R. Zhao, B. Qian, X. Lv, and P. Zhang, "Domain knowledge guided deep learning with electronic health records," in *ICDM*, 2019.
- [19] J. Luo, M. Ye, C. Xiao, and F. Ma, "HiTANet: hierarchical time-aware attention networks for risk prediction on electronic health records," in *ACM SIGKDD*, 2020.
- [20] E. Choi, M. T. Bahadori, E. Searles, C. Coffey, M. Thompson, J. Bost, J. Tejedor-Sojo, and J. Sun, "Multi-layer representation learning for medical concepts," in *ACM SIGKDD*, 2016.
- [21] E. Choi, Z. Xu, Y. Li, M. W. Dusenberry, G. Flores, Y. Xue, and A. M. Dai, "Learning the graphical structure of electronic health records with graph convolutional transformer," in *AAAI*, 2020.
- [22] T. Mikolov, I. Sutskever, K. Chen, G. S. Corrado, and J. Dean, "Distributed representations of words and phrases and their compositionality," in *NIPS*, 2013.
- [23] I. M. Baytas, C. Xiao, X. Zhang, F. Wang, A. K. Jain, and J. Zhou, "Patient subtyping via time-aware LSTM networks," in *ACM SIGKDD*, 2017.
- [24] E. Choi, C. Xiao, W. F. Stewart, and J. Sun, "MiME: multilevel medical embedding of electronic health records for predictive healthcare," in *NeurIPS*, 2018.
- [25] L. Ma, C. Zhang, Y. Wang, W. Ruan, J. Wang, W. Tang, X. Ma, X. Gao, and J. Gao, "ConCare: personalized clinical feature embedding via capturing the healthcare context," in *AAAI*, 2020.
- [26] H. Mei and J. Eisner, "The neural hawkes process: A neurally self-modulating multivariate point process," in *NIPS*, 2017.
- [27] Y. Wang, H. Shen, S. Liu, J. Gao, and X. Cheng, "Cascade dynamics modeling with attention-based recurrent neural network," in *IJCAI*, 2017.
- [28] A. Bojchevski and S. Günnemann, "Deep gaussian embedding of attributed graphs: Unsupervised inductive learning via ranking," in *ICLR*, 2018.
- [29] J. Tang, M. Qu, M. Wang, M. Zhang, J. Yan, and Q. Mei, "LINE: large-scale information network embedding," in *WWW*, 2015.
- [30] P. Guttorp, "An Introduction to the Theory of Point Processes (D. J. Daley and D. Vere-Jones)," *SIAM Review*, vol. 32, 1990.